Journal of Pharmaceutical and Biomedical Analysis 53 (2010) 98–102

Contents lists available at ScienceDirect

Journal of Pharmaceutical and Biomedical Analysis

journal homepage: www.elsevier.com/locate/jpba

Metabonomics study of the protective effects of *Lonicera japonica* extract on acute liver injury in dimethylnitrosamine treated rats

Changhai Sun[a,b], Yang Teng[a], Guangzhi Li[a], Saburo Yoshioka[b], Junko Yokota[b], Mitsuhiko Miyamura[b,*], Hongzhuang Fang[a], Yu Zhang[a]

[a] *Department of Pharmacy, Jiamusi University, Heilongjiang Province 154007, China*
[b] *Department of Pharmacy, Kochi Medical School Hospital, Kohasu, Oko-cho, Nankoku, Kochi 783-8505, Japan*

ARTICLE INFO

Article history:
Received 19 January 2010
Received in revised form 7 March 2010
Accepted 11 March 2010
Available online 17 March 2010

Keywords:
Metabonomics
Dimethylnitrosamine (DMN)
GC/MS
Hepatic injury
Lonicera japonica extract (LJE)

ABSTRACT

A metabonomics approach, consisting of gas chromatography coupled to mass spectrometry (GC/MS) and a multivariate statistical technique, was developed to estimate the protective effects of *Lonicera japonica* extract (LJE) on acute liver injury. A high dose of dimethylnitrosamine (DMN) was used to induce an acute stage of hepatic injury in 21 male Wistar rats. The rats were divided into three groups: normal, model and treatment. Pathological changes, particularly fibrosis, were also examined by Azan staining. The results indicate that clear and consistent biochemical changes occur. Nine candidate biomarkers for DMN treatment and LJE intervention under controlled conditions were identified using chemometric analysis. Pathological analysis suggests that LJE has a protective effect to the liver. This work suggests that a metabonomics approach can be used to estimate pharmacodynamic action of naturally occurring drugs in a dynamic and non-invasive way.

1. Introduction

Many chemicals that are inhaled or swallowed can induce acute liver injury [1]. Hepatic injury at the intermediate and crucial stage is characterized by reversibility. If treated properly at this stage, cirrhosis can be successfully prevented. Preventing cirrhosis and controlling cirrhosis progression remain problematic, and significant efforts have been made to find safe and effective anti-cirrhosis drugs. Despite a lack of convincing clinical evidence of effectiveness, herbal medicines have become popular among patients with liver disease and are attractive as putative antifibrotics or hepatotherapeutics [2–5].

Honeysuckle is the flower of *Lonicera japonica* Thunb, which is widely planted in China. It is one of the best-known traditional Chinese medicinal herbs and is typically used to treat common colds and fevers. A number of compounds isolated from *Lonicera* species [6,7], including organic acids, flavonoids, iridoid glycosides, and saponins, are known to be responsible for a variety of biological activities associated with *Lonicera* (e.g., hepatoprotective, cytoprotective, antimicrobial, antioxidative, antiviral and anti-inflammatory effects) [8–10]. However, the protective and antifibrotic effects of *L. japonica* against acute liver injury have not been demonstrated. When traditional methods are used to examine pathological liver changes and to estimate the protective effects of therapeutics against liver injury, the experimental animals must be sacrificed. Consequently, it is not possible to determine the dynamics of the therapeutic under study. The establishment of a non-invasive and dynamic method for estimating the protective effects of therapeutics would be significant.

Metabonomics, one of the '-omics' technologies involving modern chemical instrumentation and chemometrics analysis, is used to characterize the biochemical pattern of endogenous metabolic composition in biological samples. Metabonomic approaches are ideal for detecting a physiopathological response to a drug-, toxin- or disease-induced disturbance in an endogenous metabolic network. Thus, metabonomics is an increasingly important tool that has been successfully used to evaluate drug toxicity [11–15] and to make disease diagnoses [16–18]. In pharmaceutical research, modeling of metabolic and physiological responses to physiopathological stimuli can be important for connecting molecular events occurring at the gene and protein level to those occurring at the macro-system level, including pathological end-points [19]. Much of the original work on the estimation of drug efficacy was performed using nuclear magnet resonance (NMR) spectroscopy [13,20,21], but the sensitivity of NMR spectroscopy is generally low. In addition, the literature for estimating the efficacy of natural medicines by metabonomic methods is limited. Due to its high sensitivity, simplicity, and use in most modern databases, a combination of mass spectroscopy and chromatographic techniques, such GC/MS, is now used by many investigators to detect

* Corresponding author.
E-mail address: schai1974@sohu.com (M. Miyamura).

0731-7085/$ – see front matter © 2010 Elsevier B.V. All rights reserved.
doi:10.1016/j.jpba.2010.03.015

subtle fluctuations in endogenous metabolite concentrations [22,23].

In this study, an integrated GC/MS based metabonomic approach was used to screen and identify metabolic perturbations associated with dimethylnitrosamine (DMN) induced hepatic lesions in Wistar rat urine. A seven-day investigation was performed in order to identify the time-dependent characteristics of the metabolic response after a single DMN injection. Through the detection of metabolic difference of rat urine analyzed by GC/MS, we aimed to: (i) estimate the protective contribution of *L. japonica* extract (LJE) against liver injury, (ii) emphasize the ability of GC/MS technology as a practical and powerful tool for tracking an initial metabolic response, (iii) profile urinary biomarkers of DMN in an induced hepatotoxic model, and (iv) suggest a non-invasive complementary approach for the identification of several metabolites in any toxicological model investigation and/or for the estimation of the efficacy of natural drugs.

2. Experimental

2.1. Reagents and chemicals

Ethanol, acetonitrile, n,n-dimethylformamide (DMF), bis-(trimethylsilyl) trifluoroacetamide (BSTFA) and DMN were purchased from Wako Chemical, Ltd. (Osaka, Japan).

2.2. Preparation of LJE

L. japonica Thunb (honeysuckle) was collected from Dongaxian, Shandong Province (China), identified by Professor Hongzhuang F., and dried well in the sun. The dried honeysuckle (10 g) was powdered in a blender equipped with a refrigerator at 1000 rev min^{-1} and extracted 2 h by stirring with a mixer at 300 rev min^{-1} in 200 mL of 75% ethanol. After filtration, the supernatant was collected and evaporated under vacuum to afford 4.28 g of dried extract. The dried extract was diluted in 50 mL water and the diluted solution was stored in a refrigerator until administration to animals.

2.3. Treatment of rats

Six-week-old male Wistar rats were purchased from SLC, Inc., Japan. The animals were kept in a specific pathogen-free animal facility and were maintained at a temperature of 19–25 °C, a humidity level of 30–70%, and a 12 h day–night cycle throughout the study. Free access to pellet food and drinking water was provided throughout the study period. The experiments were conducted in accordance with the Guiding Principles for the Care and Use of Laboratory Animals. The study protocol was approved by the Animal Experimental Committee of Kochi Medical School.

Rats weighing 200–250 g (n = 21) were adapted to a semi-synthetic diet. After an initial acclimation period of 2 weeks in cages, the animals were transferred to individual metabolism cages and allowed to acclimatize for an additional 24 h. The animals were divided into a treatment group (n = 7, treated with 2 g/kg body weight of LJE each day for 14 days and one dose of 35 mg/kg body weight of DMN on day 7); a model group (n = 7, treated with oral saline solution each day and one dose of 35 mg/kg body weight of DMN on day 7); and a normal group (n = 7, treated only with oral saline solution each day). Samples of 24 h urine were collected at days 1, 3, 5 and 7 pre-dose and 1, 3, 5, and 7 post-dose after DMN injection. All collected urine samples were immediately stored at −80 °C pending GC/MS analysis. After the final collection time point, all animals were sacrificed by decapitation after halothane anesthesia and subjected to autopsy. The livers were removed immediately and stored at −80 °C.

2.4. Urine sample preparation

1.5 mL of acetonitrile was added to each urine sample (1.5 mL). The mixtures were placed in a 4 °C centrifuge and shaken for 1 h with subsequent centrifugation at 10,000 rpm. The supernatant (100 μL) was placed in a new tube and vacuum dried for 12 h. 100 μL n,n-dimethylformamide (DMF) and 50 μL bis-(trimethylsilyl) trifluoroacetamide (BSTFA) was added to each sample after drying. The mixture was dissolved by vortex apparatus and placed in 80 °C water bath to hydrolyze. After 0.5 h hydrolyzation then 10 min cooling and re-dissolving, the sample was analyzed.

2.5. GC/MS analysis

Samples of 1 μL were analyzed in a gas chromatograph with a mass selective detector (Model QP5050A, GC/MS Shimadzu), using a fused-silica capillary column (DB-1 column 60 m × 0.32 mm, film

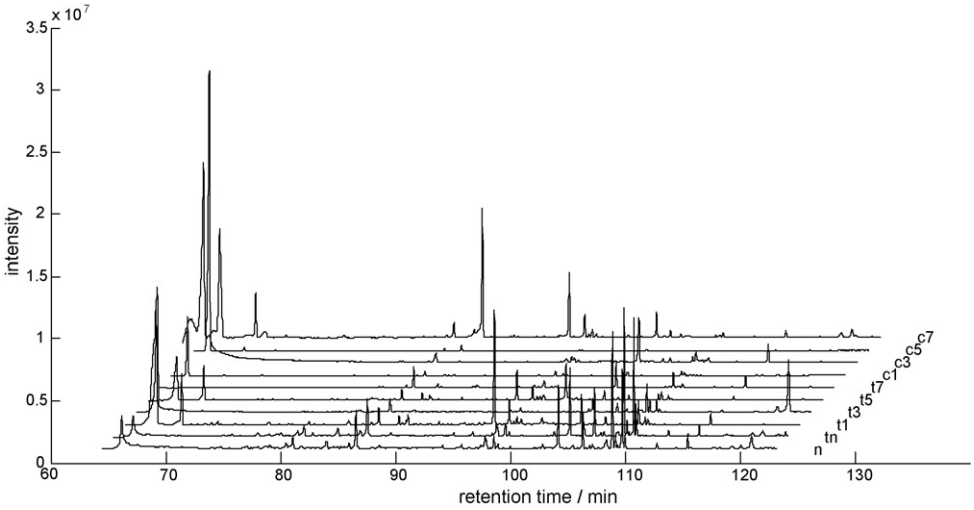

Fig. 1. Comparison of GC/MS total ion current (TIC) (40–500 m/z) chromatograms of urine sampled from rats treated with saline solution only (n), treated with extracts of *Lonicera japonica* (tn), treated with DMN but no *Lonicera japonica* extract (c1, c3, c5 and c7), and treated with DMN and *Lonicera japonica* extract (t1, t3, t5 and t7) n: the normal group; tn: the treatment group from 1 to 7 day before injected DMN; c1, c3, c5 and c7: the model group at 1, 3, 5 and 7 day after injected DMN; t1, t3, t5 and t7: the treat group at 1, 3, 5 and 7 day after injected D.

thickness 0.1 μm) in the split injection mode (1:15). The oven temperature program was as follows: 2 min at the initial temperature of 80 °C and then an increase to 90 °C at a rate of 1.0 °C min^{-1}, 10 min at 90 °C and then an increase to 108 °C at a rate of 2.0 °C min^{-1}, 10 min at 108 °C and then an increase to 110 °C at a rate of 2.0 °C min^{-1}, 10 min at 110 °C and then an increase to 285 °C at a rate of 2.5 °C min^{-1}, and 10 min at 285 °C. Other instrumental parameters were as follows: the electron energy was 70 eV, the ion source temperature was 300 °C and the injector temperature was 280 °C. Helium, as a carrier gas, was set to a column flow rate of 1 mL min^{-1}. All data were collected in the full scan mode (40–500 *m*/*z*). The dwell time for each scan was set to 100 ms.

2.6. Data processing and pattern recognition

All collected urine samples were analyzed with the above method. Each sample was represented by a GC/MS total ion current (TIC) chromatogram ranging from 40 to 500 *m*/*z*. The chromatograms of the model group were selected for comparison, and software developed with MATLAB (version 7.0.1, Mathwork Inc.) was used to process the chromatograms. Among the chromatograms, 19 peaks with a signal to noise ratio greater than 10 were found (Fig. 1 and Table 1). These peaks were used to construct a 19-dimensional vector for characterization of the urine biochemical pattern. Each vector was normalized by the MATLAB "*z*-score" function to partially account for concentration differences which are due to variations in the volume of extracted urine. Principal component analysis (PCA), the most-commonly used algorithm in metabonomic studies, was employed to process the GC/MS data using the software developed in MATLAB. The simultaneous comparison of a large number of complex variables was facilitated by a dimensional reduction via two-dimensional (the first principal component (PC1) vs. the second principal component (PC2)) mapping procedures and the output displayed with score plots, which represented the distribution of samples in multivariate space. The score plots of the first two or three principal components allow for visualization of the data and for the determination of whether any intrinsic drug-induced difference in the metabolite concentration of the urine samples exists. Finally, mean values of the peak descriptors were calculated for urine samples from drug-induced liver injury in rats at each time point and plots of PC1 vs. PC2 with mean values were generated.

2.7. Histological examination

As the final experiment, the livers were removed immediately after sacrifice and wet weighed. The liver specimens were fixed in 10% neutral buffered formalin, dehydrated, and paraffin-embedded for histochemical analysis.

3. Results and discussions

3.1. GC/MS analysis of urine samples

Fig. 1 depicts the GC/MS TIC chromatogram of urine sampled from the normal group, the model group, the treatment group before DMN injection, and the treatment group after DMN injection. The chromatogram only contains retention times of 60–125 min because there was no change in the first 60 min. The peaks considered to be representative chemical fingerprints of endogenous metabolites, which describe the metabolic perturbation induced by DMN and the protective effect of LJE on acute liver injury, are summarized in Table 1. While significant differences between the TIC profile of the model, treatment and normal groups were observed, no obvious differences between the normal and treatment groups before DMN injection were found.

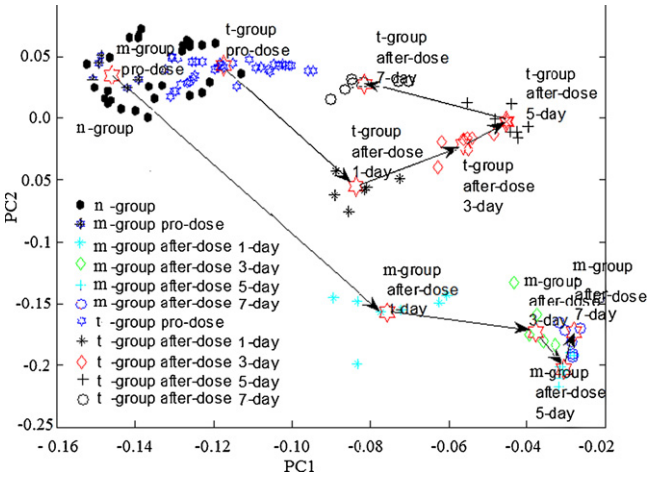

Fig. 2. Score plot of principal components derived from the GC/MS profiles of urine samples obtained from rats with no treatment (n-group), injected with DMN (m-group) and provided the extraction of *Lonicera japonica* (t-group). The plot depicts a time-dependent trajectory of metabolic patterns at different time points The n-group: the normal group samples; the t-group pre-dose: treatment group from 1 to 7 days before injected DMN; the m-group after-dose 1, 3, 5, 7-day: the model group after injected DMN at 1, 3, 5 and 7 day; t-group after-dose 1, 3, 5, 7-day: treat group after injected DMN at 1, 3, 5 and 7 day.

The enormous potential of metabonomics as a tool for the identification of novel biomarkers of toxicity has been recognized for some time. The identification of biomarkers in mammalian urine via non-invasive metabonomic analysis would be particularly valuable. Lin et al. found 11 biomarkers of liver injury in the urine of CCl_4 treated rats: citric acid, hippuric acid, taurine, L-isoleucine, creatinine, L-threonine, L-serine, beta-alanine, L-histidine, L-arginine and L-lysine [24]. No biomarkers of DMN induced liver injury are found in the literature, however.

We found that the peak areas of 3 metabolites (8-phenyl-8-azbicyclo [4.3.0] non-3-ene-7,9-dione; 2-(6-heptynyl)-1,3-dioxolane, and bis (o-methyloxime)-4-ketoglucose) significantly increased after DMN injection and that LJE could inhibit the DMN induced production of these metabolites (Table 1). On the other hand, we also found that the peak areas of 6 metabolites (malonic acid, 2-(4-chlorophenylthiomethoxy)ethyl, tetrahydro-2-furanacetaldehyde, D-galactose; erythro-pentonic acid, and galacturonic acid) significantly decreased after DMN injection and that LJE could inhibit the DMN induced reduction of these metabolites. While these 9 metabolites are candidate biomarkers of acute live injury induced by DMN and protected against by LJE, their mechanisms are not known and require further investigation.

3.2. Identification of biochemical effects

The time-course of the metabolic disturbance (Fig. 2) can be used to identify the time points of maximum biochemical effect of DMN treatment with and without LJE treatment. The normal and the pre-dose treatment groups showed little tendency for separation and no obvious difference in their metabolic patterns were found. The post-dose model and treatment groups represent the model and treatment groups, respectively, after DMN injection on day 7. On the first day, the markers representing the model and treatment groups shifted away from the markers of the normal group, with the model group shifting further than the treatment group. The shift pattern suggests that different metabolic responses occur due to the DMN interference and the LJE pro-

Table 1
The retention time, the name of components, the area and its standard differential of peaks for the biomarkers (the number of tn and n is 49, and others is 7).

No.	Rt.	Component	Area ± SD (10^{+6})									
			n	tn	t1	t3	t5	t7	c1	c3	c5	c7
1[a]	64.95	8-Phenyl-8-azbicyclo[4.3.0]non-3-ene-7,9-dione	0 ± 0.91	0.2178 ± 0.065	3.530 ± 9.33	61.32 ± 42.55	0 ± 0	0.3152 ± 0.01	379.7 ± 63.06	238.1 ± 47.59	438.4 ± 31.40	373.6 ± 28.45
2	64.95	3-[1,3]Dioxolan-2-yl-4-methoxy-6-nitro-benzo[d]isoxazole	102.9 ± 57.70	49.24 ± 48.21	51.17 ± 10.49	316.8 ± 161.6	1.946 ± 0.40	21.00 ± 5.69	33.16 ± 5.73	371.0 ± 73.12	0 ± 0	0 ± 0
3	65.83	(E)-2-(5,5,5-Trichloro-3-penten-1-yl)-1,3-dioxolane	28.97 ± 16.76	13.43 ± 4.52	433.0 ± 191.7	26.89 ± 4.20	239.9 ± 72.6	5.917 ± 2.01	4.911 ± 2.80	103.9 ± 22.51	0 ± 0	0 ± 0
4	67.81	2-(Methoxyimino)-hexanedioic acid	2.515 ± 0.27	2.009 ± 0.60	0.2419 ± 0.06	0.4079 ± 0.16	0 ± 0	1.370 ± 1.01	2.961 ± 2.83	9.292 ± 8.68	27.53 ± 34.25	28.45 ± 14.33
5	68.37	Gamma-lactone-2-methoximine-gluconic acid	1.185 ± 0.30	1.454 ± 0.50	57.96 ± 26.76	0.1353 ± 0.05	65.79 ± 48.57	1.138 ± 1.01	0 ± 0	4.156 ± 1.23	0 ± 0	0.06501 ± 0.017
6	87.47	3,3-Diphenyl-cyclopropene	92.6 ± 22.74	62.78 ± 17.10	16.64 ± 2.68	32.35 ± 19.1	55.50 ± 26.19	49.90 ± 30.10	14.88 ± 7.77	3.475 ± 2.61	0.3858 ± 0.085	3.297 ± 1.94
7[a]	89.61	2-(6-Heptynyl)-1,3-dioxolane	0 ± 0	0 ± 0	0.2223 ± 0.05	0 ± 0	10.37 ± 9.97	1.369 ± 0.62	10.32 ± 5.73	8.337 ± 2.05	77.89 ± 38.03	80.93 ± 28.60
8[a]	97.97	Bis(o-methyloxime)-4-ketoglucose	0 ± 0	0 ± 0	0 ± 0	0 ± 0	0 ± 0	0 ± 0	3.908 ± 2.34	3.469 ± 2.17	33.82 ± 22.60	35.07 ± 22.92
9	98.52	Undecanedioic acid	0 ± 0	0 ± 0	106.7 ± 49.1	56.31 ± 40.94	0 ± 0	0 ± 0	56.7 ± 49.1	46.31 ± 40.94	10.7 ± 9.1	16.31 ± 4.94
10	100.0	2-Keto-d-gluconic acid	33.99 ± 17.87	29.05 ± 12.30	21.56 ± 8.66	9.835 ± 4.01	35.22 ± 17.96	19.93 ± 13.60	12.09 ± 4.32	0.08076 ± 0.21	1.115 ± 1.48	3.986 ± 1.12
11	103.2	2-Phenylpyrido[3,4-d]-1,3-oxazin-4-one	0 ± 0	0 ± 0	4.437 ± 2.13	0 ± 0	55.57 ± 7.29	0 ± 0	0 ± 0	0 ± 0	0 ± 0	0 ± 0
12[b]	106.9	Malonic acid	144.7 ± 31.63	106.5 ± 21.81	32.77 ± 6.15	41.71 ± 27.57	70.09 ± 23.98	81.63 ± 34.53	22.39 ± 8.63	37.85 ± 7.96	1.103 ± 0.57	4.813 ± 1.27
13[b]	109.2	2-(4-Chlorophenylthiomethoxy)ethyl	90.22 ± 39.10	105.5 ± 38.89	12.50 ± 6.29	18.84 ± 12.05	11.29 ± 8.53	70.74 ± 25.04	0 ± 0	0 ± 0	0 ± 0	0 ± 0
14[b]	112.1	Tetrahydro-2-furanacetaldehyde	237.3 ± 76.55	146.2 ± 69.93	29.36 ± 9.75	74.93 ± 42.79	17.63 ± 10.64	91.78 ± 48.26	13.41 ± 3.18	0.4354 ± 0.15	1.322 ± 0.73	4.597 ± 2.03
15[b]	112.4	D-Galactose	26.02 ± 7.44	18.77 ± 6.26	20.93 ± 5.05	15.01 ± 1.41	40.72 ± 21.95	20.91 ± 21.82	14.36 ± 5.54	4.797 ± 2.04	1.341 ± 0.63	4.275 ± 1.50
16[b]	113.0	Erythro-pentonic acid	201.5 ± 52.66	215.5 ± 36.04	21.94 ± 9.36	41.29 ± 31.79	26.56 ± 14.68	155.2 ± 34.73	1.254 ± 0.88	0 ± 0	0 ± 0	0.2582 ± 0.50
17[b]	113.2	Galacturonic acid	25.11 ± 5.18	20.22 ± 2.45	3.501 ± 1.11	5.435 ± 5.47	9.495 ± 1.75	14.58 ± 4.83	2.294 ± 1.91	0 ± 0	0 ± 0	0.5045 ± 0.090
18	119.3	Malic acid	17.36 ± 7.04	10.61 ± 7.12	5.178 ± 2.44	2.890 ± 4.93	24.05 ± 16.11	13.72 ± 7.82	2.496 ± 2.50	5.956 ± 1.80	0 ± 0	0.0773 ± 0.020
19	122.7	Talonic acid	13.55 ± 54.81	24.35 ± 13.72	14.25 ± 35.40	85.89 ± 50.39	10.32 ± 5.96	26.48 ± 4.29	5.097 ± 2.60	0 ± 0	0.4632 ± 0.69	1.902 ± 1.02

n: The normal group (n = 49); tn: the treat group (n = 49) 1–7 days before injection with DMN; c1, c3, c5 and c7: the model group (n = 7) 1, 3, 5 and 7 days after injection with DMN; t1, t3, t5 and t7: the treatment group (n = 7) 1, 3, 5 and 7 days after injection with DMN. The components identified by NIST database.

[a] Biomarkers that increased with DMN treatment.

[b] Biomarkers that decreased with DMN treatment.

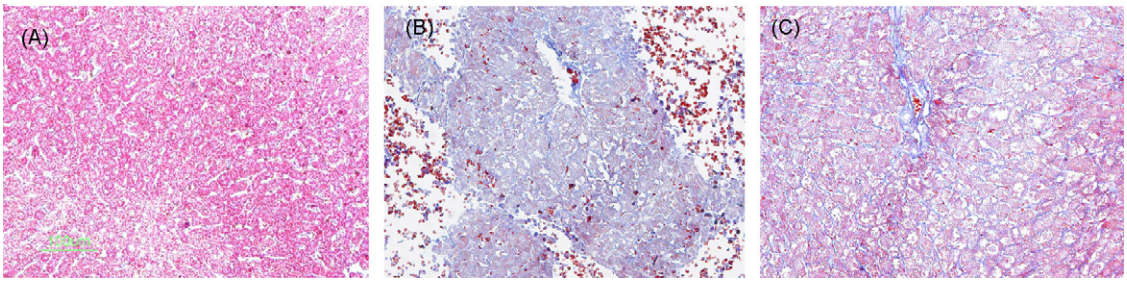

Fig. 3. Micrographs of rat liver specimens for (A) normal, (B) model, and (C) treatment groups.

tective effect against liver injury by DMN. Days 3–7 provide an indication of the progression of the metabolic disturbance through time. The maximum biochemical effect achieved by DMN was at day 5 (Fig. 2) for LJE treatment group, due to the protective effect of LJE. In contrast, the maximum biochemical effect of the model group did not occur until day 7. Fig. 2 also includes the time-dependent trajectory of metabolic patterns in the model group and the treatment group at different time points after DMN treatment. In the PCA map, each spot represents a sample, and each assembly of samples indicates a particular metabolic pattern at different time points. The locus marked by arrows represents the mean metabolic pattern changing in the time. The starting point was the principal component's mean value of the sample group collected pre-dose. The biochemical metabolic patterns changed with time and all markers at different time points demonstrated distinct difference from the sample collected pre-dose (Fig. 2). The trajectory distance of the model group was greater than that of the treatment group. Furthermore, the markers of the treatment group approached the normal group on day 7, while the model group was significantly displaced from the normal group on day 7. These results suggest that the metabolic pattern of the treatment group experienced lower fluctuations than the model group and that the normal metabolic network was restored at day 7 for the LJE treatment group, leading to a stable pattern approaching the pre-dose group.

3.3. Histopathological observations

To evaluate collagen fibers in the liver, liver sections collected from DMN-treated and untreated rats were stained with Azan staining. The livers of the untreated normal group contained only a few fibers (Fig. 3A), while the livers of the model group had increased levels of collagen and contained bundles of collagen fibers around the lobules, forming large fibrous septa (Fig. 3B). The thickening of the collagen fiber bundles was markedly reduced in the LJE treatment group (Fig. 3C). Histopathological fibrosis scores confirmed that liver fibrosis was significantly reduced in the LJE treatment group compared to the model group.

4. Conclusions

Using PCA coupled with GC/MS, we have characterized the biochemical fingerprints and physiopathologic status in an animal model. Despite a high degree of inter-subject variability in urine composition, clear and consistent biochemical changes following DMN modification were identified using PCA analysis. At the same time, 9 biomarkers for acute liver injury induced by DMN and protection by LJE were found. The results of the histopathological and the metabonomics techniques suggest that LJE has a protective effect on acute liver injury. This work demonstrates that a metabonomics approach can be used to estimate pharmacodynamic action of natural drugs in a dynamic and non-invasive way.

References

[1] E.Y. Kim, H.S. Lee, Y.J. Song, H.S. Jung, Protective effects of cuscutae semen against dimethylnitrosamine-induced acute liver injury in Sprague–Dawley rats, Biol. Pharm. Bull. 30 (2007) 1427–1431.
[2] P. Ferenci, B. Dragosics, H. Dittrich, H. Frank, L. Benda, H. Lochs, S. Meryn, W. Base, B. Schneider, Randomized controlled trial of silymarin treatment in patients with cirrhosis of the liver, J. Hepatol. 9 (1989) 105–113.
[3] M.H. Lee, S. Yoon, J.O. Moon, The flavonoid naringenin inhibits dimethyl nitrosamine-induced liver damage in rats, Biol. Pharm. Bull. 27 (2004) 72–76.
[4] D.B. Strader, B.R. Bacon, K.L. Lindsay, D.R. La Brecque, T. Morgan, E.C. Wright, J. Allen, M.F. Khokar, J.H. Hoofnagle, L.B. Seeff, Use of complementary and alternative medicine in patients with liver disease, J. Gastroenterol. 97 (2002) 2391–2397.
[5] B.E. Wang, Treatment of chronic liver diseases with traditional Chinese medicine, J. Gastroenterol. Hepatol. 15 (2000) 67–70.
[6] W.C. Chang, F.L. Hsu, Inhibition of platelet activation and endothelial cell injury by polyphenolic compounds isolated from *Lonicera japonica* Thunb, Prostaglandins Leukot. Essent. Fatty Acids 45 (1992) 307–312.
[7] W. Bors, Flavonoids asantioxidants: determination of radical-scavenging efficiencies, Methods Enzymol. 186 (1990) 343–355.
[8] I. Morel, Antioxidant and iron-chelating activities of the flavonoids catechin, quercetin and diosmetin on iron-loaded rat hepatocyte cultures, Biochem. Pharmacol. 45 (1993) 13–19.
[9] S.J. Kim, Effect of biflavones of *Ginkgo biloba* against UVB-induced cytotoxicity in vitro, J. Dermatol. 28 (2001) 193–199.
[10] O.H. Kang, Inhibition of trypsininduced mast cell activation by water fraction of *Lonicera japonica*, Arch. Pharm. Res. 27 (2004) 1141–1146.
[11] R.J. Mortishire-Smith, Use of metabonomics to identify impaired fatty acid metabolism as the mechanism of a drug-induced toxicity, Chem. Res. Toxicol. 17 (2004) 165–173.
[12] N.J. Waters, Integrated metabonomic analysis of bromobenzene-induced hepatotoxicity: novel induction of 5-oxoprolinosis, J. Proteome Res. 5 (2006) 1448–1459.
[13] M. Coen, E.M. Lenz, J.K. Nichloson, I.D. Wilson, F. Pognan, J.C. Lindon, An integrated metatonomic investigation of acetaminophen toxicity in the mouse using NMR spectroscopy, Cem. Res. Toxicol. 16 (2003) 295–303.
[14] M.E. Bollard, Comparative me-tabonomics of differential hydrazine toxicity in the rat and mouse, Toxicol. Appl. Pharmacol. 204 (2005) 135–151.
[15] N.J. Waters, Metabonomic deconvolution of embedded toxicity: application to thioacetamide hepato- and nephrotoxicity, Chem. Res. Toxicol. 18 (2005) 639–654.
[16] J.T. Brindle, Rapid and non-invasive diagnosis of the presence and severity of coronary heart disease using ^{1}H NMR-based metabonomics, Nat. Med. 8 (2002) 1439–1444.
[17] M.A. Constantinou, Application of nuclear magnetic resonance spectroscopy combined with principal component analysis in detecting inborn errors of metabolism using blood spots: a metabonomic approach, Anal. Chim. Acta 511 (2004) 303–312.
[18] O. Beckonert, Visualizing metabolic changes in breast-cancer tissue using ^{1}H NMR spectroscopy and self-organizing maps, NMR Biomed. 16 (2003) 1–11.
[19] J.K. Nicholson, Metabonomics: a platform for studying drag toxicity and gene function, Nat. Rev. Drug Discov. 1 (2002) 153–161.
[20] D.G. Robertson, M.D. Reily, R.E. Sigler, D.F. Wells, D.A. Paterson, T.K. Braden, Metabonomics: evaluation of nuclear magnetic resonance and pattern recognition technology for rapid in vivo screening of liver and kidney toxicants, Toxicol. Sci. 57 (2000) 326–337.
[21] T.M. Ebbels, E. Holmes, J.C. Lindon, J.K. Nicholson, Evaluation of metabolic variation in normal rat strains from a statistical analysis of ^{1}H NMR spectra of urine, J. Pharm. Biomed. Anal. 36 (2004) 823–833.
[22] O. Fiehn, Metabolomics: the link between genotypes and phenotypes, Plant Mol. Biol. 48 (2002) 155–171.
[23] I.D. Wilson, High resolution "ultra performance" liquid chromatography coupled to oa-TOF mass spectrometry as a tool for differential metabolic pathway profiling in functional genomic studies, J. Proteome Res. 4 (2005) 591–598.
[24] Y.P. Lin, D.Y. Si, Z.P. Zhang, C.X. Liu, An integrated metabonomic method for profiling of metabolic changes in carbon tetrachloride induced rat urine, Toxicology 256 (2009) 191–200.